Light Metals 2014
Edited by: John Grandfield
TMS (The Minerals, Metals & Materials Society), 2014

EFFECT OF TIN ON THE CORROSION AND ELECTROCHEMICAL BEHAVIOR OF Al-Zn-Mg ALLOY IN SEA WATER

M.M.Sadawy[1], K.M.Zohdy[2]

[1] Mining and Petroleum Engineering Department; Al-Azhar University; Nasr City; Cairo, 11371, Egypt
[2]Higher Technological Institute, 10th of Ramadan City, Egypt

Keywords: Al-Zn-Mg alloys, Corrosion, Polarization, Pitting, Electrochemical impedance spectroscopy

Abstract

The effect of tin on the corrosion and electrochemical behavior of Al-Zn-Mg alloy in 3.5 wt.% NaCl solution was investigated by open-circuit potential measurements (OCP), polarization techniques and electrochemical impedance spectroscopy (EIS). The Morphology of the alloy after corrosion was studied by scanning electron microscopy (SEM). The results showed that the anodic dissolution of Al-Zn-Mg alloy increased with increasing tin content. EIS measurements showed that the polarization resistance decreases with increasing tin content. Moreover, surface analysis indicated that Sn reduced intergranular corrosion of the aluminum alloy and promoted the formation of the corrosion products.

Introduction

Lightweight alloys are the key materials for the future of manufacturing industry and their use in the field of automotive, aerospace and electronics are of major research interest [1-3].

Al–Zn-Mg base alloys have been widely used as structural materials due to attractive combined properties, such as low density, high strength, ductility, toughness and resistance to fatigue [4-10]. In these alloys the high solubility of Mg and Zn in aluminum is exploited to obtain a tensile strength that pure Al does not have. In such applications Mg and Zn contribute to the alloy hardening with the formation of Guinier–Preston (GP) zones [11] and precipitates [12] which modify the aluminum lattice by internal strain so that the motion of dislocations is hampered, thus strengthening the alloy [11]. These alloys have also been considered as galvanic anode due to their anodic dissolution process showing a more negative or active corrosion potential [13].

It is known that small additions of various alloying elements often change the morphology, spatial distribution and size of precipitates. For this reason, many studies focused on improving the mechanical and corrosion properties of Al alloys to achieve excellent corrosion resistance and mechanical properties, needed for industrial applications by adding small additions of various alloying elements [14,15]. To inhibit recrystallization and to improve localized corrosion via the formation of new dispersoids in Al–Zn–Mg–Cu alloy have recently aroused lots of interest among researchers. Addition of Sc to Al–Zn–Mg–Cu alloys can produce Al_3Sc dispersoids, effectively restrain recrystallization and improve the stress corrosion resistance. Additions of Sc and Zr to Al–Zn–Mg–Cu alloys can produce finer and more stable $Al_3(Sc,Zr)$ dispersoids, and more effectively restrain recrystallization. However, expensive Sc limits the development and application of Sc-containing Al–Zn–Mg–Cu alloys. Additions of cheaper rare earth elements and transition elements to Al–Zn–Mg–Cu alloys to form new dispersoids inhibiting effectively recrystallization are being studied [7].

Another cheaper addition could be Sn, which has been tried in Al-Cu alloys and has been reported to yield remarkable property improvement by influencing the precipitate density, morphology and interfacial energy. Addition of Sn in Al-Zn-Mg alloy has shown remarkable improvement in properties and a recent report by Ogura [15] has revealed that Sn significantly reduces the precipitate free zone (PFZ) in the system without the threat of early melting owing to lower melting point of Sn. Sn has been considered as an attractive element for its interaction with a vacancy in the Al matrix and is expected to change the precipitate morphology in the vicinity of grain boundaries. However, no results have been reported on the corrosion and electrochemical behavior of Al-Zn-Mg alloy containing different amount of Sn. In the present study, the influence of Sn on the corrosion behavior of Al–5.3Zn–2.4Mg in 3.5 wt.% NaCl solution was investigated by using open-circuit potential measurements (OCP), polarization techniques and electrochemical impedance spectroscopy (EIS).

Experimental Work

Material

The present study was carried out using Al-Zn-Mg alloy. Its chemical composition is 5.3 wt.% Zn, 2.4 wt.% Mg, 0.02 wt.% Cu, 0.01 wt.% Fe and Al is the rest. Sn was added with different amount (0.05, 0.1 and 0.2 wt. %) to molten Al-Zn-Mg alloy and mechanically stirred for 5 minutes at 750˚C under a constant flux of nitrogen. The melt is then casted into steel mold of dimensions (100x50x10 mm) and naturally cooled down to room temperature.

Electrochemical Measurements

All electrochemical measurements were carried out using electrochemical work station, Gamry PCI300/4 Potentiostat/ Galvanostat / Zra analyzer, with a personal computer. Specimens were polished to 1200 grit sizes and then specimens were cleaned with distilled water. A three-electrode cell composed of a specimen as a working electrode, Pt counter electrode, and Ag/AgCl reference electrode were used for the tests. Prior to electrochemical tests, the specimens were cathodically cleaned for 15 min at -1200 mV (Ag/AgCl) to remove the air-formed oxide film. Polarization tests were carried out at a scan rate of 0.5 mV/min at 25 °C. Specimens with exposed surface area of 1.0 cm^2 were used as a working electrode. The Echem Analyst 5.21 statistically fits the experimental data to the Stern-Geary model for a corroding system. The routine automatically selects the data that lies within the Tafel region (±250 mV with respect to the corrosion potential).

The Echem Analyst calculates corrosion potential, corrosion current density, anodic and cathodic slopes.

Cyclic polarization measurements were carried out by sweeping linearly the potential from the starting potential into the positive direction at a given scan rate till a required potential value and then reversed with the same scan rate till the starting potential to form one complete cycle.

In EIS technique a small amplitude ac signal of 10mV and frequency spectrum from 100 kHz to 0.01 Hz was impressed at the OCP and impedance data were analyzed using Nyquist plots. The charge transfer resistance, R_t, was extracted from the diameter of the semicircle in Nyquist plot.

Surface Examination Study

Al-Zn-Mg specimens were immersed in 3.5 wt. %. NaCl solution for a period of 3 days. After that, the specimens were taken out and dried. The surface of the metal specimens was analyzed by scanning electron microscope (SEM, Joel-JXA-840A).

Results and Discussions

Open Circuit Potential Measurements

The electrochemical behavior of Al–5.3Zn–2.4Mg with different amount of Sn in 3.5 wt. % NaCl solutions was studied on the basis of the change in OCP with time and represented in Figure 1. Inspection of the data reveals that the OCP of Al–5.3Zn–2.4Mg, in all cases, tends from the moment of immersion towards more negative value. This behavior represents the break down of the pre-immersion air formed oxide film on Al-Zn-Mg surface. Moreover Figure 1 indicates that the OCP shifts to more negative values with increasing Sn amount. This is due to increasing amount of Sn leads to an increase in free Sn and intermetallic compounds which encourage galvanic corrosion with the surrounding matrix.

.

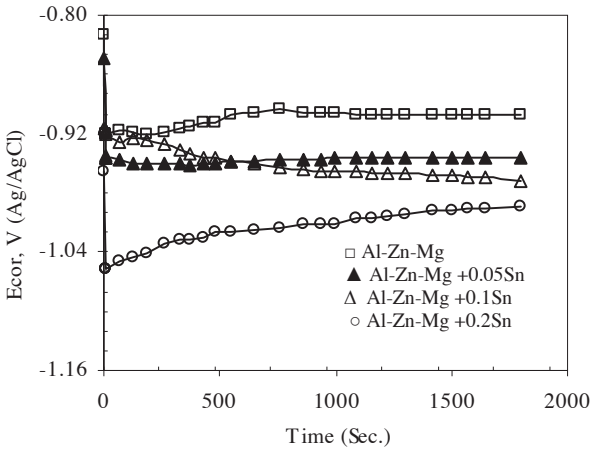

Figure 1. Potential–time curves for Al-Zn-Mg with different amount of Sn in 3.5wt. % NaCl solution.

Potentiodynamic Polarization Measurements

Figure 2 shows the potentiodynamic curves of Al-5.3Zn-2.4Mg alloy with and without Sn . It can be seen that the corrosion potential (E_{cor}) shifts to more active potential with increasing Sn in Al-5.3Zn-2.4Mg alloy. The electrochemical parameters including corrosion potential (E_{cor}), corrosion current density (i_{cor}), anodic and cathodic slopes (β_a and β_c) were calculated from Tafel plots, and are summarized in Table I.

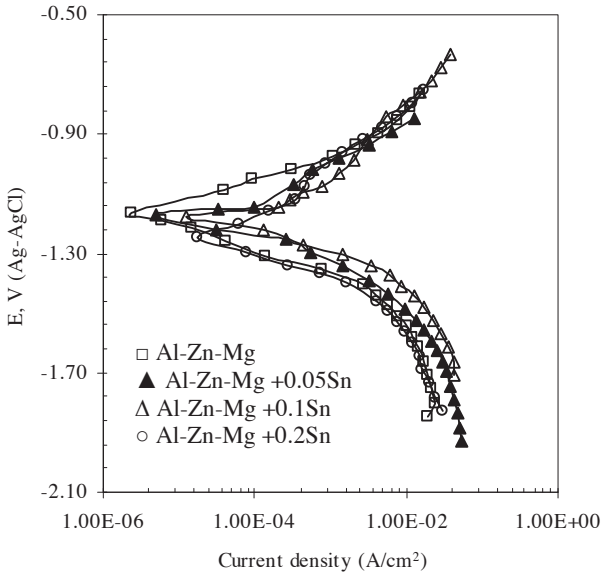

Figure 2. Anodic and cathodic polarization curves of Al-Zn-Mg with different amount of Sn in 3.5 wt. % NaCl solution.

From the calculated corrosion current densities it can be seen that the corrosion current densities increases with the increase of Sn content. From physical metallurgy and phase diagrams of aluminum alloys, it is clear that tin is negligibly soluble in aluminum. Tin has been observed to have a solubility of less than 0.01 wt.% in the aluminum matrix at the melting point of approximately 231.2 ^{0}C. Also it is known that the solubility of tin is approximately about 0.1% at temperature of 600 ^{0}C and above [16]. This is probably why its globules were found (black dots) in the aluminum matrix. It is suspected that galvanic cells set up between the tin globules and the aluminum matrix results in dissolution of aluminum or zinc and magnesium in the vicinity of the tin when they are soaked in seawater. The consequence of this phenomenon is that the networks of the passive oxides of the aluminum alloy are broken down thus increasing the anodic dissolution. [16]. Moreover Table I illustrated that the anodic and cathodic Tafel slopes were changed with increasing Sn amount. This means that Sn affects on anodic and cathodic reaction mechanisms.

Table I. Electrochemical Parameters Obtained from Potentiodynamic Polarization Measurements for the Corrosion of Al-5.3Zn-2.4Mg with Different Amount of Sn in 3.5 wt. % NaCl Solution

Sn Wt.%	$E_{cor.}$ (V)	i_{cor} (A/cm^2)	β_c (V/dec)	β_a (V/dec)
0.0	-1.16	$4.1*10^{-5}$	0.38	0.24
0.05	-1.18	$9.5*10^{-5}$	0.43	0.28
0.1	-1.23	$2.8*10^{-4}$	0.55	0.30
0.2	-1.34	$4.6*10^{-4}$	0.56	0.35

Cyclic Polarization Measurements

Pitting studies were conducted by cyclic polarization technique. Figure 3 (a and b) presents cyclic polarization curves recorded for Al-Zn-Mg alloy with and without Sn content in 3.5 wt. % NaCl solution. The solid arrows next to the forward and the reverse anodic branches indicate potential scan directions.

Cyclic polarization technique allows the repassivation potential (E_{rp}) to be determined. In the present work, E_{rp} is defined as the potential on the reverse scan at which the anodic current becomes zero (i.e., the current changes polarity). Determination of E_{rp} is essential in order to establish the passive and pitting potential regions of the system. Indeed, in pitting corrosion studies, E_{rp} is the relevant potential instead of E_b because significant induction time for pit nucleation may exist when the potential is increased from the passive region. At potentials more negative than E_{rp}, the electrode is protected by an oxide film and pitting will only take place at more positive potentials [17]. This remarkable hysteresis anodic loop denotes that Al was able to repassivate after the breakdown of the passive film. It is obvious from Fig. 3(a) that the obtained plots had the familiar form for Al and Al alloys showing a well-defined corrosion potential, E_{cor}, followed by a passive region. The passive region results due to the formation of a protective barrier oxide film.

On the other hand cyclic polarization curves indicate that smaller content of Sn does not affect the pitting potential. The pitting potential tends to become more negative with increasing Sn content. A more negative potential signifies an easier breakdown of oxide film. The characteristic parameters associated to cyclic polarization curves are summarized in Table II.

Electrochemical Impedance Spectra

EIS studies were carried out to get information about the electrochemical and physico-chemical phenomena associated with the electrode reactions during dissolution process. The EIS plots of Al–Zn–Mg with and without Sn are shown in Figures 4 and 5(a and b). The high spectra are used to detect the local surface defects, whereas the medium and low frequency spectra detect the processes within the corrosion product and at the metal/corrosion product interface, respectively. The Nyquist plots for all samples in Figure 4 presented a single capacitance loop in the whole frequency range, which indicates that the system can be described by a single time constant model. The high frequency plot has been associated with the charge transfer process and the low frequency plot with mass transfer process. Moreover, the presence of single time constant in the spectra can be observed from the phase angle at low frequencies as shown in Figure 5b. According to the Bode plots of |Z| versus frequency shown in Figure 5a, it was found that the |Z| for as-received sample was the maximum value, and then it reduced gradually with the increase of Sn content.

The characteristic parameters associated to the impedance diagram (R_s, R_p and C_{dl}) are given in Table III. Where, R_s is the solution resistance, R_p represents the charge transfer resistance of the interfacial reaction and C_{dl} is the capacitance. As seen from Table III, the value of (R_p) decreases and C_{dl} increases with an increasing Sn content. A decrease in the capacitance, which can result from increase in the thickness of the oxide film. The equivalent circuit used to fit the behavior of Al-5.3Zn-2.4Mg with different amount of Sn in 3.5wt. % NaCl solution is shown in Figure 6.

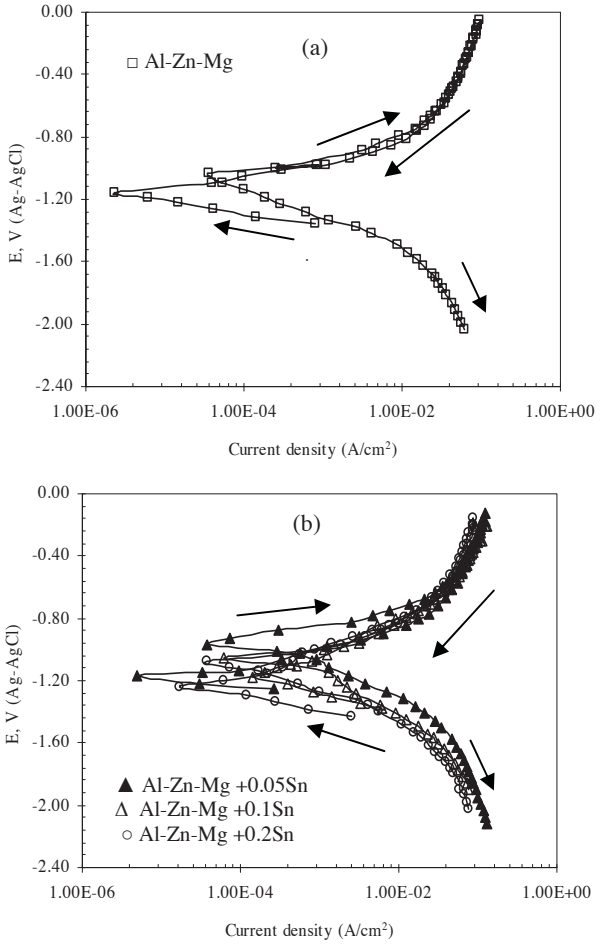

Figure 3. Cyclic polarization curves of as-received Al-5.3Zn-2.4Mg (a) and Al-5.3Zn-2.4Mg with Sn additions (b) in 3.5 wt. % NaCl solution.

Table II. Cyclic Polarization Parameters of Al-5.3Zn-2.4Mg in 3.5 3.5wt. % NaCl Solution with and without Sn

Sn Wt.%	$E_{cor.}$ (V)	E_{pit} (V)	E_{rp} (V)
0.0	-1.16	-0.047	-1.01
0.05	-1.18	-0.129	-0.970
0.1	-1.23	-0.150	-0.980
0.2	-1.34	-0.170	-1.00

Table III. Effect of Sn Additions on the Electrochemical Impedance Parameters of Al-5.3Zn-2.4Mg in 3.5wt. % NaCl Solution

Sn Wt.%	R_s (Ω cm^2)	R_p (Ω cm^2)	C_{dl} (μF/cm^2)
0.0	3.51	229.2	30.4
0.05	3.50	222.4	40.2
0.1	3.50	162.3	55.4
0.2	3.50	152.1	65.6

Surface Morphology

The corrosion surface morphology of the investigated alloy with and without Sn addition after constant immersion time for 3 days was observed using scanning electron microscopy (SEM) as shown in Figure 7(a-d).

Figure 7(a and b) shows the surface of as-received and 0.05wt. % Sn alloys. The corrosion product is minimal but the attack seems to be along grain boundaries. This is due to in the as-cast condition there is existence of a microstructure consisting of α-Al solid solution with precipitation of the τ (Al-Zn-Mg) phase and an eutectic consisting of a fine dispersion of the α and τ segregates (α + τ) at grain boundaries as shown in Figure 8.

On the other hand Figure 7(c and d) represents the micrographs of samples with 0.1 and 0.2 wt.% Sn .This Figure illustrates the breakdown of oxide film and corrosion product layer are found on the alloys. The amount of corrosion product layer increases with increasing Sn content. This is due to increasing Sn content, the precipitates are uniformly distributed throughout the whole grain and encouraged breakdown of the passive oxide network.

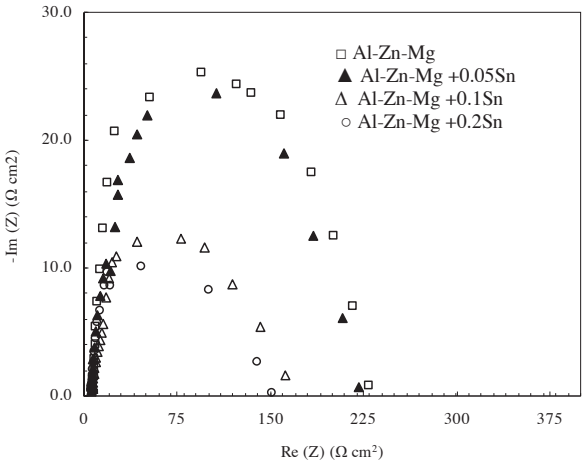

Figure 4. Nyquist plots of Al-5.3Zn-2.4Mg with different amount of Sn in 3.5wt. % NaCl solution.

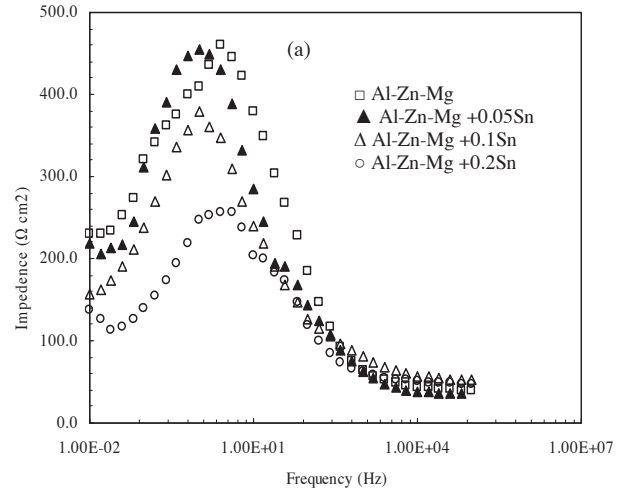

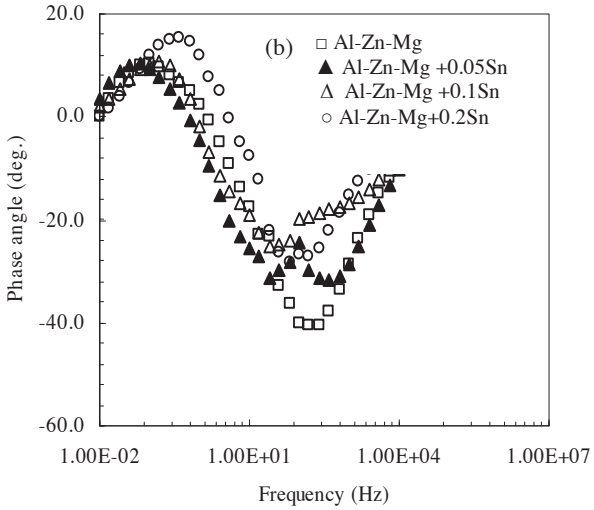

Figure 5(a and b). Bode plots of Al-5.3Zn-2.4M with different amount of Sn in 3.5wt. % NaCl solution.

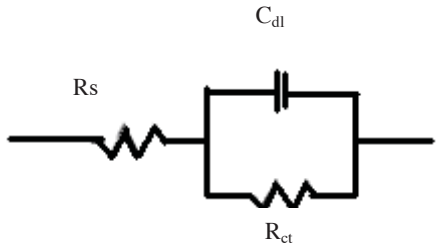

Figure 6. The equivalent circuit used to fit the behavior of Al-5.3Zn-2.4Mg with different amount of Sn in 3.5wt. % NaCl solution.

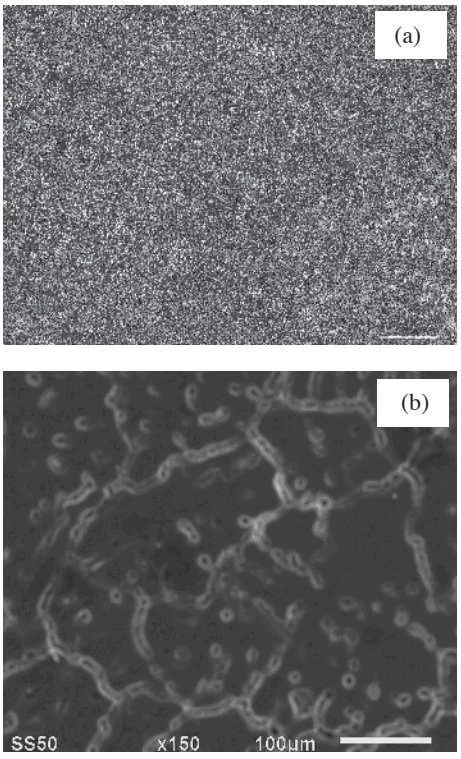

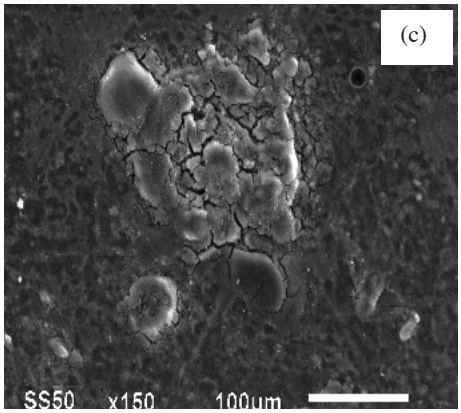

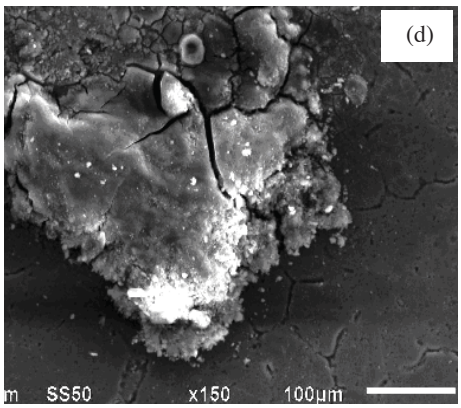

Figure 7. SEM micrographs of surface morphology of samples tested after constant immersion in 3.5 wt.% NaCl for 3 days, (a) 0 wt.% , (b) 0.05 wt.%, (c), 0.1wt.% and (d) 0.2 wt.% Sn.

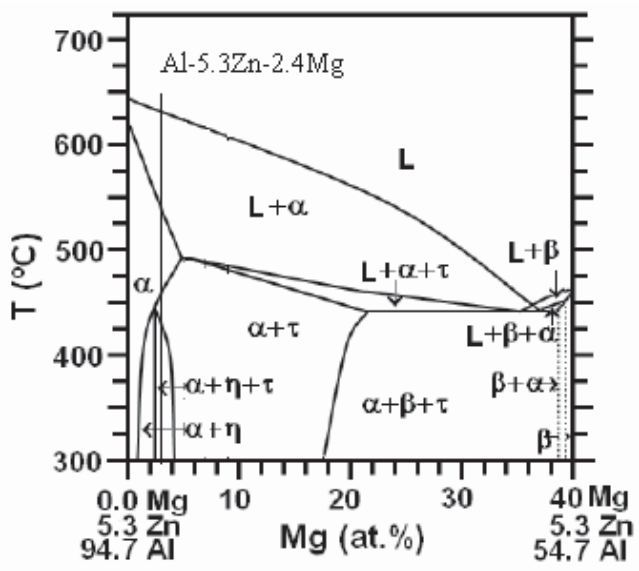

Figure 8. Vertical section of the ternary Al–Zn–Mg phase diagram [18,19]. The vertical line shows the composition of the investigated alloy.

Conclusions

The effect of tin Additions on the corrosion and electrochemical behavior of Al–Zn–Mg alloy was studied. The results showed that:

1. The corrosion potential shifts to more active potential and the corrosion current density increases with increasing tin additions.
2. The pitting potential tends to become more negative with increasing Sn content.
3. SEM analysis showed that the investigated alloy with Sn content up to 0.05 wt. % is easily corroded along the grain boundaries whilst further addition of Sn promoted uniform corrosion.
4. The amount of corrosion product layer increases with increasing Sn content.

References

1. N. D. Nama et al., "Effect of Manganese Additions on the Corrosion Behavior of an Extruded Mg–5Al based Alloy," *Journal of Alloys and Compounds,* 542 (2012), 199–206.
2. L. Agrawal, and R. Yadav A. Sexena,"Effect of Magnesium Content on the Mechanical Properties of Al-Zn-Mg Alloys,"*International Journal on Emerging Technologies,* 3(1)(2012), 137-140.
3. A.H. Feng and Z.Y. Ma, ," Enhanced Mechanical Properties of Mg–Al–Zn Cast Alloy via Friction Stir Processing,"*Scripta Materialia,* 56 (2007), 397–400.
4. A.V. Sameljuk , et al., "Effect of Rapid Solidification on the Microstructure and Corrosion Behaviour of Al–Zn–Mg Based Material," *Corrosion Science,* 49 (2007) , 276–286.
5. A.V. Sameljuk et al., "Corrosion Behaviour of Powder Metallurgical and Cast Al–Zn–Mg Base Alloys," *Corrosion Science,* 46 (2004), 147–158.
6. F.Andreatta , H.Terryn, and J.H.W. Wit , "Effect of Solution Heat Treatment on Galvanic Coupling Between Intermetallics and Matrix in AA7075-T6," *Corrosion Science,* 45 (2003), 1733–1746.
7. H.C. Fang, et al., "Effect of Cr, Yb and Zr Additions on Localized Corrosion of Al–Zn–Mg–Cu Alloy," *Corrosion Science,* 51 (2009), 2872–2877.
8. F. Andreatta , H. Terryn, and J.H.W. Wit, "Corrosion Behaviour of Different Tempers of AA7075 Aluminium Alloy," *Electrochimica Acta,* 49 (2004), 2851–2862.
9. A.V. Benedetti , et al., "Effect of Welding on the Microstructure and Electrochemical Corrosion of Al–Zn–Mg–Fe Alloys," *Electrochimica Acta,* 45 (2000), 2187–2195.
10. G. Peng, et al., "Effect of Cr and Yb Additions on Microstructure and Properties of Low Copper Al–Zn–Mg–Cu–Zr Alloy," *Materials and Design,* 36 (2012) , 279–283.
11. W. Xue et al., ,"Corrosion Behaviors and Galvanic Studies of Microarc Oxidation Films on Al–Zn–Mg–Cu Alloy," *Surface & Coatings Technology,* 201 (2007), 8695–8701.
12. A. Barbucci et al., "Role of intermetallics in the activation of Al–Mg–Zn alloys," *Journal of Alloys and Compounds,* 268 (1998) 295–301.
13. S. Valdez et al., "Microhardness, Microstructure and Electrochemical Efficiency of an Al (Zn/xMg) Alloy after Thermal Treatment,"*Journal of Material Science Technology*, 28(3)(2012), 255–260.
14. D.W. Suh et al., "Microstructural Evolution of Al–Zn–Mg–Cu–(Sc) Alloy During Hot Extrusion and Heat Treatments,"

Journal of Materials Processing Technology, 155–156 (2004), 1330–1336.
15. T. Ogura et al., " Effects of Microalloying Tin and Combined Addition of Silver and Tin on the Formation of Precipitate Free Zones and Mechanical Properties in Al-Zn-Mg Alloys," *Materials Transactions*, 52 (5) (2011), 900 – 905.
16. L.E. Umoru and O.O. Ige, " Effects of Tin on Aluminum – Zinc – Magnesium Alloy as Sacrificial Anode in Seawater *Journal of Minerals & Materials Characterization & Engineering",* 7(.2)(2007), 105-113.
17. M. A. Amin , S. S. Abd El Rehim and A.S. El-Lithy , "Pitting and Pitting Control of Al in Gluconic Acid Solutions – Polarization, Chronoamperometry and Morphological Studies,"*Corrosion Science,* 52 (2010), 3099–3108.
18. M. A. Suarez et al., "The Effect of Mg Content on Microstructure in Al 12wt. %Zn - x Mg Alloy," *Journal of Applied Research and Technology,* 7(1) (2009), 153-162.
19. O. Alvarez et al., "Characterization and Prediction of Microstructure in Al Zn–Mg Alloys," *Materials Science and Engineering A* 402 (2005), 320–324.